

Neutral-current neutrino-nucleus quasielastic scattering

Andrea Meucci, Carlotta Giusti, and Franco Davide Pacati

*Dipartimento di Fisica Nucleare e Teorica, Università di Pavia and
Istituto Nazionale di Fisica Nucleare, Sezione di Pavia, I-27100 Pavia, Italy*

A relativistic distorted-wave impulse-approximation model to quasielastic neutral-current neutrino-nucleus scattering is developed, using the relativistic mean field theory for the bound state and taking into account the final state interaction in the relativistic scattering state. Results for the neutrino (antineutrino) reaction on ^{12}C target nucleus are presented in an energy range between 500 and 1000 MeV. The sensitivity to the strange quark content of the axial-vector form factor is discussed.

PACS numbers: 25.30.Pt 13.15.+g 24.10.Jv

I. INTRODUCTION

The neutral-current scattering of neutrinos and antineutrinos on nucleons and nuclei has gained in recent years a wide interest in order to determine the structure of hadronic weak neutral current. In a measurement of the proton spin structure function, the European Muon Collaboration [1] found out a disagreement with the Ellis-Jaffe sum rule [2], when only up and down quark and antiquark contribution to the proton spin was taken into account, thus indicating that other flavors might contribute to the spin structure of the proton. A measurement of neutrino (antineutrino)-proton elastic scattering at Brookhaven National Laboratory (BNL) [3] supported this result by reporting a non-zero value for the strange axial-vector form factor of the nucleon. However, the BNL data were critically reanalyzed in Ref. [4], where also strange vector form factors were taken into account. It turned out that the BNL data cannot provide us decisive conclusions about the strange form factors [4]. The BoONE experiment [5] at Fermi National Laboratory (FermiLab) aims, through the FermiLab Intense Neutrino Scattering Scintillator Experiment (FINeSSE) [6], at performing a detailed investigation of the strangeness contribution to the proton spin via neutral current elastic scattering.

In order to reach a definite conclusion, nuclear structure effects have to be clearly understood. Quasielastic electron scattering calculations [7], which were able to successfully describe a wide number of experimental data, can provide us a useful tool to study neutrino-induced processes. However, a careful analysis of neutrino-nucleus reactions introduces additional complications, as the final neutrino cannot in practice be measured and a final hadronic probe has to be detected: the corresponding cross sections are therefore semi-inclusive in the hadronic sector and inclusive in the leptonic one.

General review papers about neutrino-nucleus interactions can be found in Refs. [8, 9, 10, 11]. The relativistic Fermi gas (RFG) model was applied to study neutral-current neutrino-induced knockout from nuclei in Ref. [12], where binding energies corrections and strange-quark axial-vector and vector effects were investigated. Detailed analyses of nuclear structure effects on the determination of strangeness contribution were performed in Refs. [13, 14]. In addition to the RFG model a “hybrid” model in which bound nucleons are described by harmonic oscillator wavefunctions was proposed in Ref. [13], while a relativistic shell model was used in Ref. [14]. The effects of final state interactions (FSI) were also studied in Ref. [15] in the framework of random phase approximation (RPA) and a continuum RPA model was developed in Ref. [16], where nucleosynthesis processes were also discussed. The FSI effects are generally large on the cross section, but they are reduced when studying the ratio of proton to neutron cross sections. This

was discussed in Refs. [12, 14, 17]. The effects of two-body relativistic meson exchange currents in neutrino-nucleus scattering at low and intermediate energies were evaluated in Refs. [18, 19]. The sensitivity of the neutrino-nucleus cross sections to the strange-quark contribution was also examined in a relativistic plane wave impulse approximation (RPWIA) in Ref. [20], where a model-independent approach based on eight structure functions was developed.

In this paper we present a relativistic distorted-wave impulse-approximation (RDWIA) calculation of neutral-current ν - and $\bar{\nu}$ -nucleus reactions in the quasielastic region, where a neutrino interacts with only one nucleon in the nucleus and the others nucleons behave as spectators. The RDWIA treatment is the same as in Refs. [21, 22, 23], where it was applied to electromagnetic knockout reactions and in Ref. [24], where a relativistic Green's function approach was developed dealing with the quasielastic charged-current ν -nucleus scattering. The relativistic bound state wave-functions are solutions of a Dirac equation containing scalar and vector potentials obtained in the framework of the relativistic mean field theory [25, 26]. The FSI are taken into account through a relativistic optical model potential [27, 28]. The effective Pauli reduction has been adopted in this case and the resulting Schrödinger-like equations are solved for each partial wave.

The formalism is outlined in Sec. II. Results are presented and discussed in Sec. III. Some conclusions are drawn in Sec. IV.

II. THE FORMALISM OF THE SEMI-INCLUSIVE QUASIELASTIC SCATTERING

The neutral-current $\nu(\bar{\nu})$ -nucleus cross section for the semi-inclusive process can be written as the contraction between the lepton tensor and the hadron tensor, i.e.,

$$d\sigma = \frac{G^2}{2} 2\pi L^{\mu\nu} W_{\mu\nu} \frac{d^3k}{(2\pi)^3} \frac{d^3p_N}{(2\pi)^3}, \quad (1)$$

where $G \simeq 1.16639 \times 10^{-11} \text{ MeV}^{-2}$ is the Fermi constant, and $k_i^\mu = (\varepsilon_i, \mathbf{k}_i)$, $k^\mu = (\varepsilon, \mathbf{k})$ are the four-momentum of the incident and final neutrino or antineutrino, respectively, and \mathbf{p}_N is the momentum of the emitted nucleon.

The lepton tensor has a similar structure as in electromagnetic knockout or in charged-current ν -nucleus scattering and can be written as in Ref. [7, 20, 24]. After projecting into the initial and the final neutrino (antineutrino) states, it is decomposed into a symmetrical and an antisymmetrical component, i.e.,

$$L^{\mu\nu} = \frac{2}{\varepsilon_i \varepsilon} [l_S^{\mu\nu} \mp l_A^{\mu\nu}], \quad (2)$$

with

$$\begin{aligned} l_S^{\mu\nu} &= k_i^\mu k^\nu + k_i^\nu k^\mu - g^{\mu\nu} k_i \cdot k \\ l_A^{\mu\nu} &= i \epsilon^{\mu\nu\alpha\beta} k_{i\alpha} k_\beta, \end{aligned} \quad (3)$$

where $\epsilon^{\mu\nu\alpha\beta}$ is the antisymmetric tensor with $\epsilon_{0123} = -\epsilon^{0123} = 1$. The upper (lower) sign in Eq. 2 refers to $\nu(\bar{\nu})$ scattering.

Here, we assume the reference frame where the z -axis is parallel to the momentum transfer $\mathbf{q} = \mathbf{k}_i - \mathbf{k}$ and the y -axis is parallel to $\mathbf{k}_i \times \mathbf{k}$.

The hadron tensor for the semi-inclusive scattering is given in its general form by bilinear combinations of the transition matrix elements of the nuclear weak neutral-current operator J^μ between the initial state $|\Psi_0\rangle$ of the nucleus, of energy E_0 , and the final states of energy E_f , given

by the product of a discrete (or continuum) state $|n\rangle$ of the residual nucleus and a scattering state $\chi_{\mathbf{p}_N}^{(-)}$ of the emitted nucleon, with momentum \mathbf{p}_N and energy E_N . It can be written as

$$W^{\mu\nu}(\omega, \mathbf{q}) = \sum_n \langle n; \chi_{\mathbf{p}_N}^{(-)} | J^\mu(\mathbf{q}) | \Psi_0 \rangle \langle \Psi_0 | J^{\nu\dagger}(\mathbf{q}) | n; \chi_{\mathbf{p}_N}^{(-)} \rangle \delta(E_0 + \omega - E_f), \quad (4)$$

where the sum runs over all the states of the residual nucleus.

Here, the transition matrix elements are calculated in the first order perturbation theory and in the impulse approximation, i.e., the incident neutrino interacts with only one nucleon, while the other ones behave as spectators. Thus, the transition amplitude is assumed to be adequately described as the sum of terms similar to those appearing in the electron scattering case [7, 21]

$$\langle n; \chi_{\mathbf{p}_N}^{(-)} | J^\mu(\mathbf{q}) | \Psi_0 \rangle = \langle \chi_{\mathbf{p}_N}^{(-)} | j^\mu(\mathbf{q}) | \varphi_n \rangle, \quad (5)$$

where $\varphi_n = \langle n | \Psi_0 \rangle$ describes the overlap between the initial nuclear state and the final state of the residual nucleus, corresponding to one hole in the ground state of the target. The single-particle current operator related to the weak neutral current is

$$j^\mu = F_1^V(Q^2)\gamma^\mu + i\frac{\kappa}{2M}F_2^V(Q^2)\sigma^{\mu\nu}q_\nu - G_A(Q^2)\gamma^\mu\gamma^5 + F_P(Q^2)q^\mu\gamma^5, \quad (6)$$

where κ is the anomalous part of the magnetic moment, $q^\mu = (\omega, \mathbf{q})$, $Q^2 = |\mathbf{q}|^2 - \omega^2$, is the four-momentum transfer, and $\sigma^{\mu\nu} = (i/2)[\gamma^\mu, \gamma^\nu]$. F_1^V and F_2^V are the isovector Dirac and Pauli nucleon form factors, taken from Ref. [29]. G_A is the axial form factor and F_P is the induced pseudoscalar form factor, which does not contribute to massless neutrino scattering. The vector form factors F_i^V can be expressed in terms of the corresponding electromagnetic form factors for protons (F_i^P) and neutrons (F_i^n), plus a possible isoscalar strange-quark contribution (F_i^s), i.e.,

$$\begin{aligned} F_i^V &= \left(\frac{1}{2} - 2\sin^2\theta_W\right) F_i^P - \frac{1}{2}F_i^n - \frac{1}{2}F_i^s \quad (\text{proton knockout}), \\ F_i^V &= \left(\frac{1}{2} - 2\sin^2\theta_W\right) F_i^n - \frac{1}{2}F_i^P - \frac{1}{2}F_i^s \quad (\text{neutron knockout}), \end{aligned} \quad (7)$$

where θ_W is the Weinberg angle ($\sin^2\theta_W \simeq 0.2313$). Standard dipole parametrization is adopted for the vector form factors [12, 29]. The axial form factor is expressed as [29]

$$\begin{aligned} G_A &= \frac{1}{2}(g_A - g_A^s)G \quad (\text{proton knockout}), \\ G_A &= -\frac{1}{2}(g_A + g_A^s)G \quad (\text{neutron knockout}), \end{aligned} \quad (8)$$

where $g_A \simeq 1.26$, g_A^s describes possible strange-quark contributions, and $G = (1 + Q^2/M_A^2)^{-2}$ with $M_A = 1.026$ GeV. The strange vector form factors are taken as [15]

$$\begin{aligned} F_2^s(Q^2) &= \frac{F_2^s(0)}{(1 + \tau)(1 + Q^2/M_V^2)^2}, \\ F_1^s(Q^2) &= \frac{F_1^s Q^2}{(1 + \tau)(1 + Q^2/M_V^2)^2}, \end{aligned} \quad (9)$$

where $\tau = Q^2/4M_p^2$, $F_2^s(0) = \mu_s$, $F_1^s = -\langle r_s^2 \rangle/6$, and $M_V = 0.843$ GeV. The quantity μ_s is the strange magnetic moment and $\langle r_s^2 \rangle$ the squared ‘‘strange radius’’ of the nucleus.

The differential cross section for the quasielastic neutral-current $\nu(\bar{\nu})$ -nucleus scattering is obtained from the contraction between the lepton and hadron tensors, as in Ref. [8]. After performing an integration over the solid angle of the final nucleon, we have

$$\frac{d\sigma}{d\varepsilon d\Omega dT_N} = \frac{G^2}{2\pi^2} \varepsilon^2 \cos^2 \frac{\vartheta}{2} \left[v_0 R_{00} + v_{zz} R_{zz} - v_{0z} R_{0z} + v_T R_T \pm v_{xy} R_{xy} \right] \frac{|\mathbf{p}_N| E_N}{(2\pi)^3}, \quad (10)$$

where ϑ is the lepton scattering angle and E_N the relativistic energy of the outgoing nucleon. The coefficients v are given as

$$\begin{aligned} v_0 &= 1 \quad , \quad v_{zz} = \frac{\omega^2}{|\mathbf{q}|^2} \quad , \\ v_{0z} &= \frac{\omega}{|\mathbf{q}|} \quad , \quad v_T = \tan^2 \frac{\vartheta}{2} + \frac{Q^2}{2|\mathbf{q}|^2} \quad , \\ v_{xy} &= \tan \frac{\vartheta}{2} \left[\tan^2 \frac{\vartheta}{2} + \frac{Q^2}{|\mathbf{q}|^2} \right]^{\frac{1}{2}} \quad , \end{aligned} \quad (11)$$

where the neutrino mass has been neglected.

The response functions R are given in terms of the components of the hadron tensor as

$$\begin{aligned} R_{00} &= \int d\Omega_N W^{00} \quad , \\ R_{zz} &= \int d\Omega_N W^{zz} \quad , \\ R_{0z} &= \int d\Omega_N 2 \operatorname{Re}(W^{0z}) \quad , \\ R_T &= \int d\Omega_N (W^{xx} + W^{yy}) \quad , \\ R_{xy} &= \int d\Omega_N 2 \operatorname{Im}(W^{xy}) \quad . \end{aligned} \quad (12)$$

Here, we are interested in the single differential cross section with respect to the outgoing nucleon kinetic energy T_N , i.e.

$$\frac{d\sigma}{dT_N} = \int \left(\frac{d\sigma}{d\varepsilon d\Omega dT_N} \right) d\varepsilon d\Omega \quad , \quad (13)$$

and in the ‘‘total’’ cross section

$$\sigma = \int \left(\frac{d\sigma}{dT_N} \right) dT_N \quad . \quad (14)$$

In the calculation of the transition amplitudes of Eq. 5 the relativistic single-particle scattering wave function is written as in Refs. [21, 30] in terms of its upper component, following the direct Pauli reduction scheme, i.e.,

$$\chi_{\mathbf{p}_N}^{(-)} = \left(\frac{1}{M + E + S^\dagger(E) - V^\dagger(E)} \Psi_{f+} \sigma \cdot \mathbf{p} \Psi_{f+} \right) \quad , \quad (15)$$

where $S(E)$ and $V(E)$ are the scalar and vector energy-dependent components of the relativistic optical potential for a nucleon with energy E [27]. The upper component, Ψ_{f+} , is related to a

two-component spinor, Φ_f , which solves a Schrödinger-like equation containing equivalent central and spin-orbit potentials and which is obtained from the relativistic scalar and vector potentials [28, 31], i.e.,

$$\begin{aligned}\Psi_{f+} &= \sqrt{D^\dagger(E)} \Phi_f, \\ D(E) &= 1 + \frac{S(E) - V(E)}{M + E},\end{aligned}\tag{16}$$

where $D(E)$ is the Darwin factor.

The single-particle overlap functions φ_n in Eq. 5 are taken as the Dirac-Hartree solutions of a relativistic Lagrangian containing scalar and vector potentials [25, 26].

III. THE RESULTS FOR ^{12}C

The calculations have been performed for the ^{12}C nucleus with the same bound state wave functions and optical potentials as in Refs. [21, 22, 23, 24, 30], where the relativistic approach was developed to study (ν_μ, μ^-) , $(e, e'p)$, (γ, p) , and (e, e') reactions.

The relativistic bound state wave functions have been obtained from Ref. [25], where relativistic Hartree-Bogoliubov equations are solved in the context of a relativistic mean-field theory and reproduce single-particle properties of several spherical and deformed nuclei [26]. The scattering state is computed by means of the energy-dependent and A-dependent EDAD1 complex phenomenological optical potential of Ref. [27], which is fitted to proton elastic scattering data on several nuclei in an energy range up to 1040 MeV. The initial states φ_n are taken as single-particle one-hole states in the target, with a unitary spectral strength. The sum runs over all the occupied states. In this way we include the contributions of all the nucleons in the nucleus, but disregard effects of correlations. These effects, however, are expected to be small on the semi-inclusive cross section, and, moreover, should not change the effects of FSI and of the strange-quark content of the form factors, which represent the main aim of the present investigation.

Calculations have been performed for three different values of the incoming $\nu(\bar{\nu})$ energy, i.e., $E_{\nu(\bar{\nu})} = 500, 700, \text{ and } 1000$ MeV. Firstly, we investigate the effects of the FSI between the emitted nucleon and the residual nucleus, which are described in our approach by means of a phenomenological optical-model potential. The cross sections calculated in RDWIA and in RPWIA are compared in Fig. 1 for proton emission and in Fig. 2 for neutron emission. A reduction of the cross sections of $\simeq 50\%$ is found in Fig. 1, similar to the one obtained in the case of electromagnetic proton knockout [7]. However, a larger reduction ($\simeq 60\%$) is obtained in Fig. 2 when a neutron is emitted. Therefore, the ratio between the cross sections for proton and neutron emission is enhanced by distortion. The comparison between the cross sections for an incident neutrino and antineutrino gives the contribution of the axial component of the neutral current. The results are in reasonable agreement with those of Ref. [20].

The effect of a strange-quark contribution to the axial-vector form factor is studied in Figs. 3 and 4, where the cross sections with $g_A^s = -0.19$ are compared with the corresponding ones without any strange-quark content in the weak current. The results with $g_A^s = -0.19$ are enhanced by $\simeq 50\%$ with respect to those with $g_A^s = 0$ in the case of proton knockout and reduced by $\simeq 30\%$ in the case of neutron knockout. This different behavior is due to the different sign of the interference term $g_A g_A^s$ in the proton and in the neutron case. The effect of g_A^s is less significant in the cross sections with an incident antineutrino.

The effect of the strange vector form factors $F_2^s(Q^2)$ and $F_1^s(Q^2)$ on the neutrino quasielastic cross sections is shown in Fig. 5. We have chosen as in Ref. [4] $F_2^s(0) = -0.40$ and $F_1^s = -\langle r_s^2 \rangle / 6 =$

0.53 GeV^{-2} . The Q^2 dependence is given in Eq. 9. While F_2^s decreases the cross sections, F_1^s gives an enhancement that, at $E_\nu = 1 \text{ GeV}$, almost cancels the effect of F_2^s . These effects are smaller than that produced by the strange axial-vector form factor, g_A^s , which is shown also in Fig. 5 for a comparison.

In order to separate the effects of the strange-quark contribution and of FSI on the cross sections, it was suggested in Refs.[12, 14, 17] to measure the ratio of proton to neutron yields, as this ratio is expected to be less sensitive to distortion effects than the cross sections themselves. Moreover, from the experimental point of view the ratio is less sensitive to the uncertainties in the determination of the incident neutrino flux. In Fig. 6 the ratio for an incident neutrino is displayed as a function of the outgoing nucleon kinetic energy. It is very sensitive to g_A^s and exhibits, for $g_A^s = -0.19$, a pronounced maximum at $T_N \simeq 0.6 E_\nu$. The RPWIA results are similar to those of Ref. [20]. A sizable enhancement of the ratio is produced by FSI. This result is mainly due to the different effects of the optical potential in proton and neutron knockout. It means that the argument of looking for the strange-quark content in this ratio is strengthened by distortion.

The global effect of the strange-quark contribution is shown in Fig. 7, where the cross sections, integrated over the emitted nucleon kinetic energy, are displayed. The cross section is increased by $\simeq 50\%$ for proton knockout and decreased by $\simeq 30\%$ for neutron knockout. The effect is smaller for the cross sections with an incident antineutrino. The ratio of proton to neutron cross sections is shown in Fig. 8. It is largely enhanced (by a factor $\simeq 2$) for neutrino scattering, and less enhanced ($\simeq 50\%$) for antineutrino scattering.

Finally, we compare our results with the data of the BNL 734 experiment [3]. Wide band neutrino and antineutrino beams of average energies of 1.3 and 1.2 GeV, respectively, were used to study neutral-current $\nu(\bar{\nu})$ -proton scattering. Approximately 80% of the events were due to quasielastic scattering from ^{12}C nuclei and 20% to elastic scattering from free protons. Experimental results were presented in the form of a flux-averaged differential cross section per momentum transfer squared Q^2 , which, for a free proton, is related to the recoil energy by the simple relation $Q^2 = 2MT_p$. In the case of quasielastic scattering on a complex nucleus, this is only approximately true. However, we can still define

$$\left\langle \frac{d\sigma}{dQ^2} \right\rangle = \frac{1}{2M} \int dT_{\nu(\bar{\nu})} \Phi(T_{\nu(\bar{\nu})}) \frac{d\sigma}{dT_p}, \quad (17)$$

where the $\nu(\bar{\nu})$ spectrum, $\Phi(T_{\nu(\bar{\nu})})$, is normalized to 1. In Fig. 9 our results for the flux-averaged cross section are displayed and compared with BNL data. The quasielastic cross sections have been weighed with the free proton scattering ones [4, 32]. We show results with $g_A^s = -0.19$ and without the strange-quark contribution. Moreover, following Ref. [4], we give the effect of including the strange vector form factors, F_1^s and F_2^s , with $F_1^s = -\langle r_s^2 \rangle / 6 = 0.53 \text{ GeV}^{-2}$, $F_2^s(0) = -0.40$, and the Q^2 dependence given in Eq. 9. The strange-quark contribution produces an enhancement of the cross sections, which makes them slightly higher than the experimental data. The strange weak magnetic contribution decreases the cross section, while the axial and weak electric components give an enhancement. In the lower panel of Fig. 9 the ratio of neutrino to antineutrino flux-averaged cross sections is presented and compared with the BNL data. The shape of the experimental data is reasonably reproduced.

IV. SUMMARY AND CONCLUSIONS

We have presented relativistic calculations for neutral current $\nu(\bar{\nu})$ -nucleus quasielastic scattering. The reaction mechanism is assumed to be a direct one: the incident neutrino (antineutrino) interacts with only one nucleon in the target nucleus and the other nucleons remain as spectators.

A sum over all single particle occupied states is performed, using an independent particle model to describe the structure of the nucleus. The scattering state is an optical-model wave function. Results for the ^{12}C target nucleus have been presented at neutrino (antineutrino) energies up to 1000 MeV. The optical potential produces a large reduction of the cross sections. The sensitivity to the strange-quark content of the axial-vector form factor has been investigated. A negative value of $g_A^s = -0.19$ sensibly increases the cross section for proton knockout and decreases it for neutron knockout. A large enhancement of the ratio of proton-to-neutron cross sections is obtained with respect to the case with $g_A^s = 0$. The enhancement is increased by FSI. The sensitivity to the strange-quark contribution of the vector form factors has also been discussed. F_2^s decreases and F_1^s enhances the cross sections. The two effects tend to cancel each other and are anyhow smaller than the effects produced by a strange axial-vector form factor. Finally, a comparison with the BNL 734 experimental data has been presented. The shape of the experimental data is reasonably reproduced.

-
- [1] J. Ashman, *et al.*, Nucl. Phys. **B328** (1989) 1.
 - [2] J.R. Ellis and R.L. Jaffe, Phys. Rev. D **9** (1974) 1444.
 - [3] L.A. Ahrens, *et al.*, Phys. Rev. D **35** (1987) 785.
 - [4] G.T. Garvey, W.C. Louis, and D.H. White, Phys. Rev. C **48** (1993) 761.
 - [5] E. Church, *et al.*, *A proposal for an experiment to measure $\nu_\mu \rightarrow \nu_e$ oscillation and ν_μ disappearance at FermiLab Booster: BooNE*, LA-UR-98-352, FermiLab experiment 898. More information may be found at <http://www-boone.fnal.gov/>.
 - [6] S. Brice, *et al.*, *A Proposal for a near detector experiment on the booster neutrino beamline: FINeSSE*, hep-ex/0402007. Additional information may be found at <http://home.fnal.gov/~bflaming/finesse.html>.
 - [7] S. Boffi, C. Giusti, F. D. Pacati, and M. Radici, *Electromagnetic Response of Atomic Nuclei*, Oxford Studies in Nuclear Physics, Vol. 20 (Clarendon Press, Oxford, 1996); S. Boffi, C. Giusti, and F. D. Pacati, Phys. Rep. **226** (1993) 1.
 - [8] J.D. Walecka, in *Muon Physics*, Vol. II, edited by V.H. Hughes and C.S. Wu (Academic Press, New York, 1975), p. 113.
 - [9] T.W. Donnelly and R.D. Peccei, Phys. Rep. **50** (1979) 1.
 - [10] W.M. Alberico, S.M. Bilenky, and C. Maieron, Phys. Rep. **358** (2002) 227.
 - [11] E. Kolbe, K. Langanke, G. Martinez-Pinedo, and P. Vogel, J. Phys. G **29** (2003) 2569.
 - [12] C.J. Horowitz, Hungchong Kim, D.P. Murdock, and S. Pollock, Phys. Rev. C **48** (1993) 3078.
 - [13] M.B. Barbaro, A. De Pace, T.W. Donnelly, A. Molinari, M.J. Musolf, Phys. Rev. C **54** (1996) 1954.
 - [14] W.M. Alberico, M.B. Barbaro, S.M. Bilenky, J.A. Caballero, C. Giusti, C. Maieron, E. Moya de Guerra, and J.M. Udías, Nucl. Phys. **A623** (1997) 471.
 - [15] G.T. Garvey, S. Krewald, E. Kolbe, and K. Langanke, Phys. Rev. C **48** (1993) 1919.
 - [16] N. Jachowicz, S. Rombouts, K. Heyde, and J. Ryckebusch, Phys. Rev. C **59** (1999) 3246.
 - [17] G.T. Garvey, S. Krewald, E. Kolbe, and K. Langanke, Phys. Lett. **B289** (1992) 249.
 - [18] Y. Umino, J.M. Udias, and P.J. Mulders, Phys. Rev. Lett. **74** (1995) 4993.
 - [19] Y. Umino and J.M. Udias, Phys. Rev. C **52** (1995) 3399.
 - [20] B.I.S. van der Ventel, and J. Piekarewicz, Phys. Rev. C **69** (2004) 035501.
 - [21] A. Meucci, C. Giusti, and F.D. Pacati, Phys. Rev. C **64** (2001) 014604.
 - [22] A. Meucci, C. Giusti, and F.D. Pacati, Phys. Rev. C **64** (2001) 064615.
 - [23] A. Meucci, Phys. Rev. C **65** (2002) 044601.
 - [24] A. Meucci, C. Giusti, and F.D. Pacati, Nucl. Phys. **A** (2004), in press [nucl-th/0311081].
 - [25] W. Pöschl, D. Vretenar, and P. Ring, Comput. Phys. Commun. **103** (1997) 217.
 - [26] G.A. Lalazissis, J. König, and P. Ring, Phys. Rev. C **55** (1997) 540.
 - [27] E.D. Cooper, S. Hama, B.C. Clark, and R.L. Mercer, Phys. Rev. C **47** (1993) 297.
 - [28] B.C. Clark, in *Proceedings of the Workshop on Relativistic Dynamics and Quark-Nuclear Physics*, edited by M.B. Johnson and A. Picklesimer (John Wiley & Sons, New York, 1986), p. 302.
 - [29] M.J. Musolf and T.W. Donnelly, Nucl. Phys. **A546** (1992) 509.

- [30] A. Meucci, F. Capuzzi, C. Giusti, and F.D. Pacati, Phys. Rev. C **67** (2003) 054601.
 [31] M. Hedayati-Poor, J.I. Johansson, and H.S. Sherif, Nucl. Phys. **A593** (1995) 377.
 [32] J.F. Beacom and S. Palomares-Ruiz, Phys. Rev. D **67** (2003) 093001.

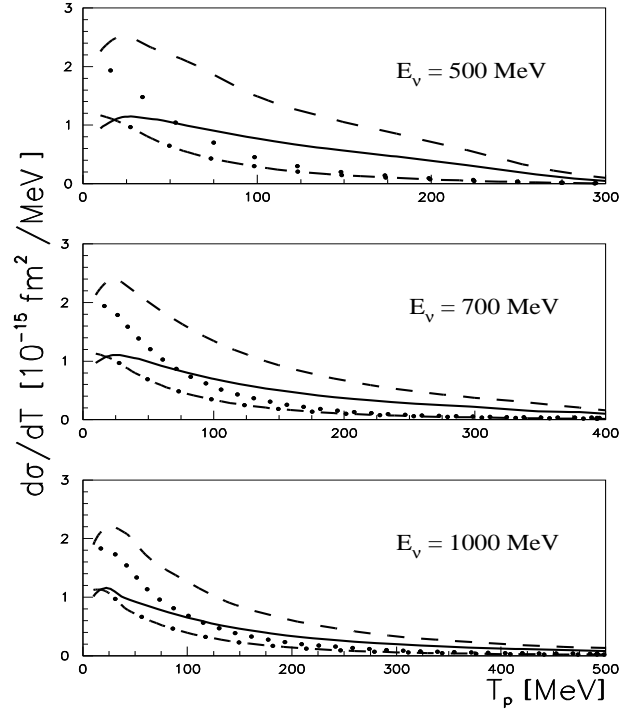


FIG. 1: Differential cross sections of the $\nu(\bar{\nu})$ quasielastic scattering on ^{12}C as a function of the outgoing proton kinetic energy T_p . Solid and dashed lines are the results in RDWIA and RPWIA, respectively, for an incident neutrino. Dot-dashed and dotted lines are the results in RDWIA and RPWIA, respectively, for an incident antineutrino. The strangeness contribution is here neglected.

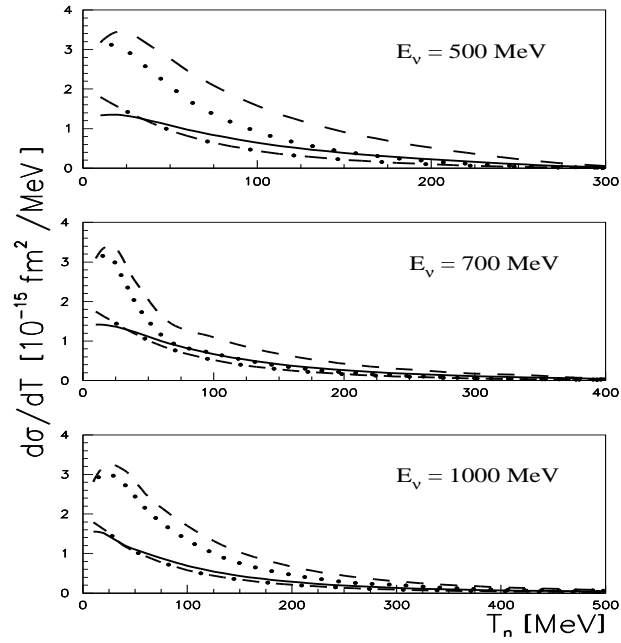


FIG. 2: The same as in Fig. 1 but for neutron knockout.

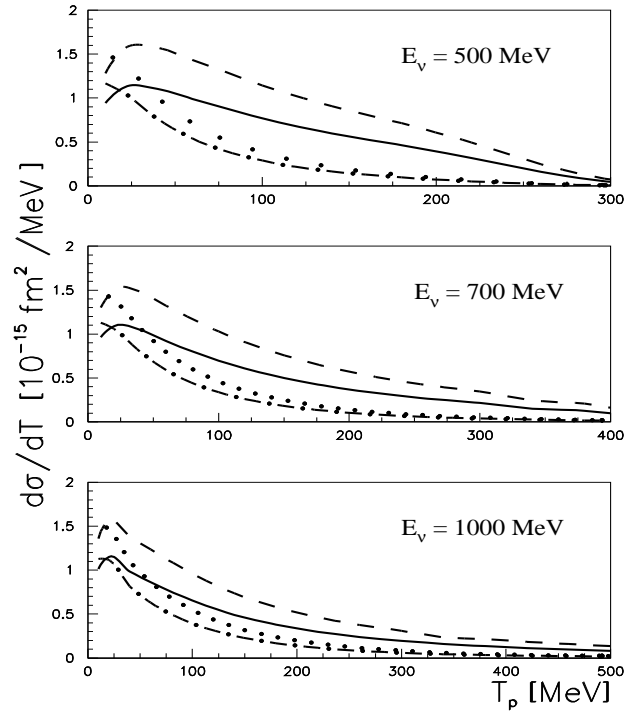


FIG. 3: Differential cross section in RDWIA of the $\nu(\bar{\nu})$ quasielastic scattering on ^{12}C as a function of the outgoing proton kinetic energy T_p . Solid and dashed lines are the results with $g_A^s = 0$ and $g_A^s = -0.19$ in the case of an incident neutrino. Dot-dashed and dotted lines are the corresponding results for an incident antineutrino.

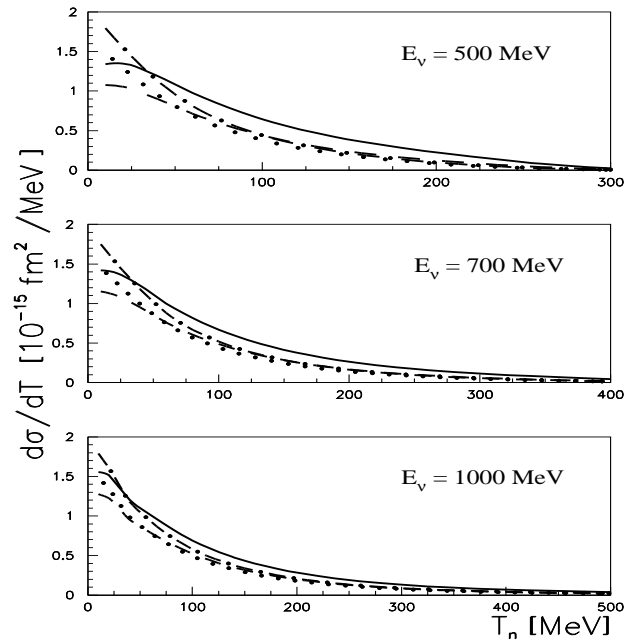


FIG. 4: The same as in Fig. 3 but for neutron knockout.

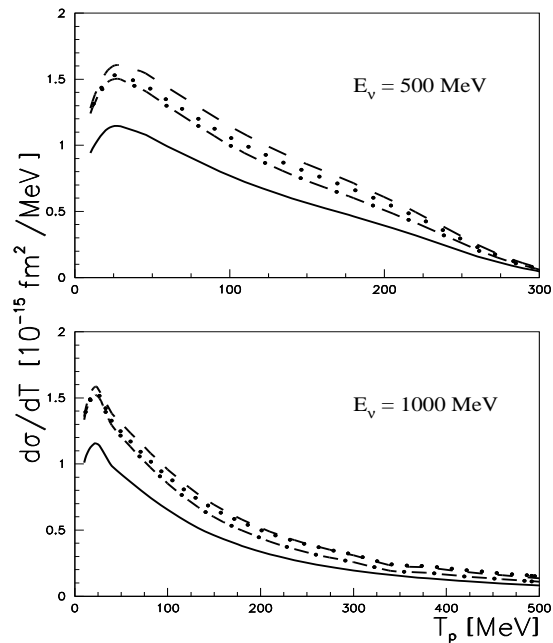


FIG. 5: Differential cross section of the ν quasielastic scattering on ^{12}C as a function of the outgoing proton kinetic energy T_p . Solid lines are the results with no strangeness contribution, dashed lines with $g_A^s = -0.19$, dot-dashed lines with $g_A^s = -0.19$ and $F_2^s(0) = -0.40$, dotted lines with $g_A^s = -0.19$, $F_2^s(0) = -0.40$ and $F_1^s = -\langle r_s^2 \rangle / 6 = 0.53 \text{ GeV}^{-2}$.

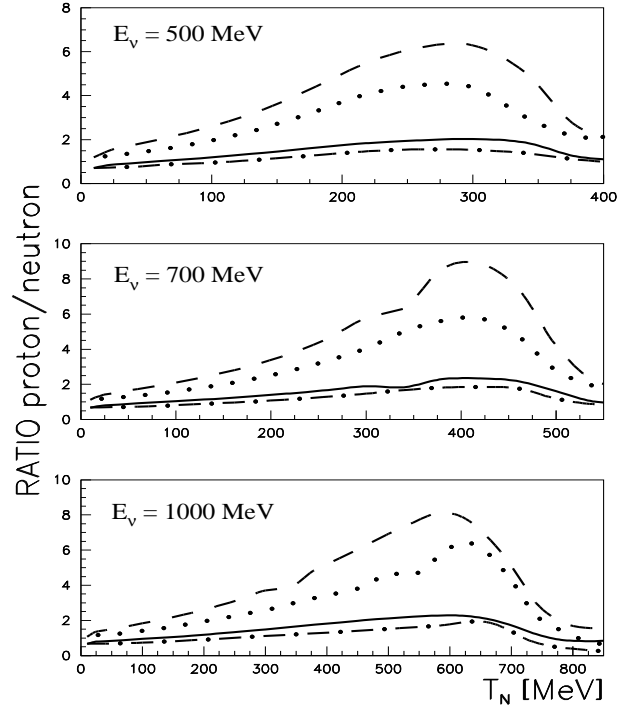


FIG. 6: Ratio of proton to neutron cross sections of the ν quasielastic scattering on ^{12}C as a function of the outgoing nucleon kinetic energy T_N . Solid and dashed lines are the results in RDWIA with $g_A^s = 0$ and $g_A^s = -0.19$. Dot-dashed and dotted lines are the same results but in PWIA.

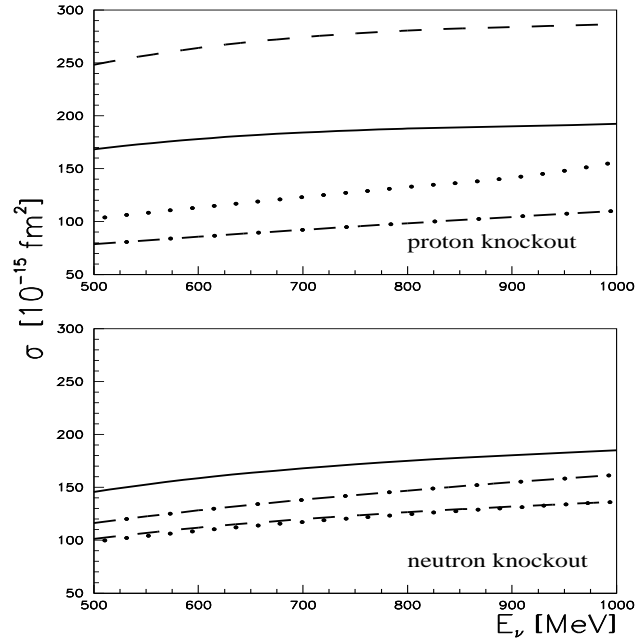


FIG. 7: The total cross section of the $\nu(\bar{\nu})$ quasielastic scattering on ^{12}C integrated over the outgoing nucleon kinetic energy. Upper panel: proton knockout. Lower panel: neutron knockout. Line convention as in Fig. 3.

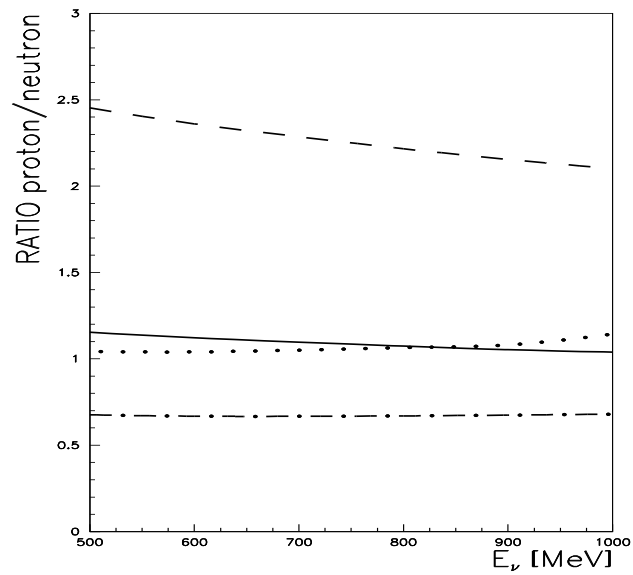


FIG. 8: Ratio of proton to neutron total cross sections of the $\nu(\bar{\nu})$ quasielastic scattering on ^{12}C as a function of the incident neutrino (antineutrino) energy. Solid and dashed lines are the results in RDWIA with $g_A^s = 0$ and $g_A^s = -0.19$. Dot-dashed and dotted lines are the same results but for an incident antineutrino.

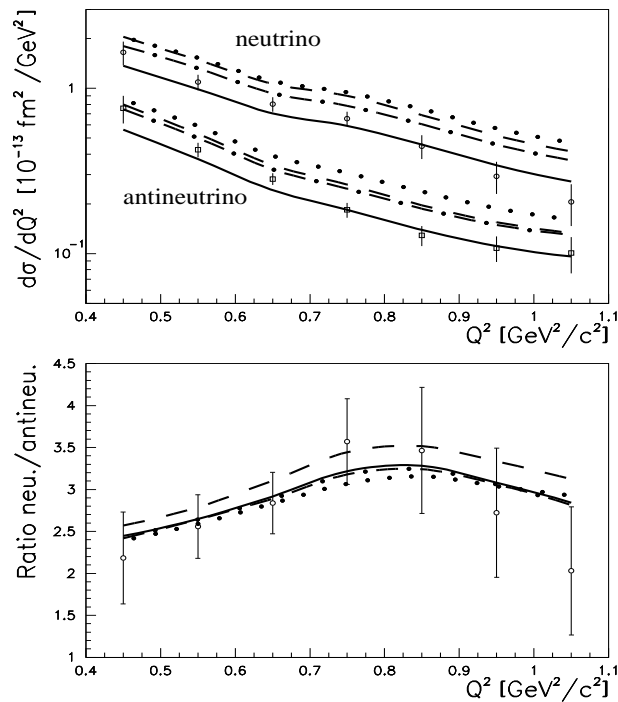


FIG. 9: Upper panel: differential cross sections of the $\nu(\bar{\nu})$ quasielastic scattering, flux-averaged over BNL spectrum [3], as a function of the momentum transfer squared. The four upper curves are for incident neutrino and the four lower ones for incident antineutrino. Lower panel: ratio of neutrino to antineutrino flux-averaged cross sections. Line convention for both panels as in Fig. 5. Experimental data from Ref. [3].